

RESEARCH ARTICLE

Frequency studies of nonlinear TSDT FGM plates in the linear shear corrections and thermal environment temperature

C.C. Hong^{1*}

¹ Hsiuping University of Science and Technology, Department of Mechanical Engineering, Taichung, Taiwan

Article History

Received 7 July 2024 Accepted 2 October 2024

Keywords

TSDT
FGM
Nonlinear
Fully homogeneous equation
Frequency

Abstract

The effects of third-order shear deformation theory (TSDT) and varied linear shear correction coefficient on the vibration frequency of thick functionally graded material (FGM) plates with fully homogeneous equations under thermal environment and power law are investigated. The nonlinear coefficient c_1 term of displacement field of TSDT is included in the fully homogeneous equation under vibration of FGM plates. The determinant of the coefficient matrix in dynamic equilibrium differential equations under vibration can be represented in the fully fifth-order polynomial equation, thus the natural frequency can be found. The natural frequency with/without the nonlinear c_1 term of displacement fields is investigated. It is a significant novelty with the consideration of the nonlinear c_1 term in the frequency computation.

1. Introduction

Some investigations in the free vibration frequency with shear deformation effect of displacement fields for the laminated, functionally graded material (FGM) plates. Abualnour et al. [1] presented a quasi-3D trigonometric displacement field theory used for the free vibration of FGM plates. Some numerical results of natural frequencies were obtained for the materials Al/Al2O3 and Al/ZrO2. Mercan et al. [2] presented a first-order shear deformation theory (FSDT) used for the free vibration of FGM/CNT (carbon nano tube) annular thick plates. Some numerical results of frequencies were obtained by using the discrete the discrete singular convolution (DSC) method. Vu et al. [3] presented a refined simple third-order shear deformation theory (R-STSDT) used for the free vibration of FGM plates. Some numerical results of natural frequencies were obtained for the thick materials Al/ZrO2 by using the mesh-free technique. Endo [4] presented the onehalf order and FSDT theory used for the exact frequency relationships of general polygonal plates. Gupta and Talha [5] presented a new hyperbolic higher-order shear and normal deformation theory (HHSNDT) used for the free vibration of FGM plates. Some numerical nonlinear and linear frequency results were obtained for the materials SUS304/Si3N4. Rezaei et al. [6] presented a simple FSDT used for the free vibration of FGM plates. Some numerical results of natural frequencies were obtained. Singh and Singh [7] presented two new trigonometric deformation theories (TDT) and trigonometric-hyperbolic deformation theory (THDT) used for the free vibration of laminated plates. Some numerical results of natural frequencies were obtained. Thai et al. [8] presented a simple higher-order shear deformation theory (HSDT) used for the

eISSN 2630-5763 © 2023 Authors. Publishing services by golden light publishing®.

^{*} Corresponding author (cchong@mail.hust.edu.tw)

free vibration of isotropic plates. Some numerical results of frequencies were obtained. Senjanovic et al. [9] presented a new FSDT used for the free vibration of moderately thick plates. Some numerical results of frequencies were obtained. Mahi et al. [10] presented a new hyperbolic shear deformation theory used for the free vibration of isotropic plates and FGM plates. Some numerical results of frequencies were obtained for the materials Al/Al2O3 and SUS304/Si3N4. Akavci [11] presented an efficient shear deformation theory used for the FGM plates in the free vibration of an electric foundation. Some numerical results of frequencies were obtained for the materials Al/Al2O3 and Al/ZrO2. Jha et al. [12] presented a higher-order shear and normal deformation theory (HOSNDT) used for the free vibration of FGM plates. Some numerical results of natural frequencies were obtained for the materials Al/ZrO2.

Some frequency investigations in the composited FGM plates of TSDT models with the effects of varied modified shear correction factors were presented. Hong [13] presented the frequency of FGM plates by considering the effects of the nonlinear varied modified shear correction factor. Hong [14] presented the frequency of FGM plates by considering the effect of a linear shear correction factor. There were a lot of published papers in this FGM area that usually used the traditional homogeneous equation without considering the effect of thermal environment temperature. The main novelty and contribution of the present work is to present the computed vibration frequency by using a fully homogeneous equation and considering the effect of thermal environment temperature on the thick FGM plates. The difference between this present study and the previous work, i.e., Ref. [13], is the type of shear correction factor. The linear shear correction coefficient type is used in [13]. It is interesting to investigate the natural frequency in the approach of the TSDT model and the varied effects of linear shear correction coefficient of FGM thick plates under vibration with fully homogeneous equations and four edges in simply supported boundary conditions. Parametric effects of the nonlinear coefficient c_1 the term, environment temperature and FGM power law index on the vibration frequency of FGM thick plates under a thermal environment are investigated.

2. Formulation

For the frequency study of a two-material thick FGM plate under thermal environment temperature T with thickness h_1 and h_2 of FGM material 1 and FGM material 2, respectively. Fig. 1 shows the geometry of two-material FGM plates under T. The material properties of the power-law function of thick FGM plates are considered in standard variation form of the power-law exponent parameter R_n . The properties in individual constituent materials are functions of T. The formula for the variation of material constants and individual properties P_i in the FGM included as follows [13]:

$$P_i = P_0(P_{-1}T^{-1} + 1 + P_1T + P_2T^2 + P_3T^3)$$
 (1)

in which P_0 , P_{-1} , P_1 , P_2 and P_3 are the temperature constants.

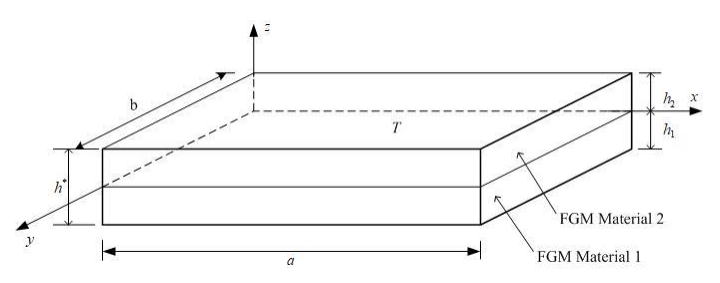


Fig. 1. Geometry of two-material FGM plates under T

The time-dependent displacements u and v of thick FGM plates are assumed to contain the displacements u^0 , v^0 on the middle-plane, shear rotations ψ_x , ψ_y and nonlinear coefficient c_1 terms of TSDT equations [13,15]. The non-linearity types of u and v are in function of z^3 with $c_1 = \frac{4}{3(h^*)^2}$ terms, in which h^* is the total thickness of FGM plates. The displacement field of TSDT is added as follows such that the transverse displacement w includes the transverse displacement on the mid-surface only.

$$u = u^{0}(x, y, t) + z\psi_{x}(x, y, t) - c_{1}z^{3}(\psi_{x} + \frac{\partial w}{\partial x})$$
 (2)

$$v = v^{0}(x, y, t) + z\psi_{y}(x, y, t) - c_{1}z^{3}(\psi_{y} + \frac{\partial w}{\partial y})$$
(3)

$$w = w(x, y, t) \tag{4}$$

where *t* is time.

The integrals of density parameters are defined as follows:

$$I_i = \sum_{k=1}^{N^*} \int_k^{k+1} \rho^{(k)} z^i dz \qquad (i=0,1,2,...,6)$$
 (5)

in which N^* is the total number of layers, $\rho^{(k)}$ is the density of kth constituent ply.

$$J_i = I_i - c_1 I_{i+2}$$
 (i=1,4)

$$K_2 = I_2 - 2c_1I_4 + c_1^2I_6 (7)$$

The integrals of stiffness parameters are given as follows.

$$(A_{i^sj^s}, B_{i^sj^s}, D_{i^sj^s}, E_{i^sj^s}, F_{i^sj^s}, H_{i^sj^s}) = \int_{\frac{-h^*}{2}}^{\frac{h^*}{2}} \bar{Q}_{i^sj^s} (1, z, z^2, z^3, z^4, z^6) dz \qquad (i^s, j^s = 1, 2, 6)$$
(8)

$$(A_{i^*j^*}, B_{i^*j^*}, D_{i^*j^*}, E_{i^*j^*}, F_{i^*j^*}, H_{i^*j^*}) = \int_{\frac{-h^*}{2}}^{\frac{h^*}{2}} k_{\alpha} \bar{Q}_{i^*j^*} (1, z, z^2, z^3, z^4, z^5) dz \qquad (i^*, j^* = 4,5)$$
(9)

where $\bar{Q}_{i^sj^s}$ and $\bar{Q}_{i^*j^*}$ are transformed reduced stiffness for FGM plates can be used in the simple forms in 2007 by Shen [16]. k_{α} is the shear correction coefficient. A short formulation for the material properties of the power-law function in FGM material gradation law is added as follows [17]:

$$E_{fgm} = (E_2 - E_1)(\frac{z + h^*/2}{h^*})^{R_n} + E_1$$
 (10)

$$v_{fgm} = (v_2 + v_1)/2 \tag{11}$$

$$\rho_{fgm} = (\rho_2 + \rho_1)/2 \tag{12}$$

$$\alpha_{fgm} = (\alpha_2 + \alpha_1)/2 \tag{13}$$

$$\kappa_{fgm} = (\kappa_2 + \kappa_1)/2 \tag{14}$$

$$C_{v_{fgm}} = (C_{v_2} + C_{v_1})/2, (15)$$

in which E is Young's modulus, ν is Poission's ratio, ρ is the density, α is the thermal expansion coefficient, κ is the thermal conductivity, C_{ν} is the specific heat. With the subscript fgm denoting the FGM plate, the

subscripts 1 and 2 denote the constituent material 1 and 2, respectively. The constituent terms of Young's modulus E_1, E_2 ; the Poission's ratio v_1, v_2 ; the density ρ_1, ρ_2 ; the thermal expansion coefficient α_1, α_2 ; the thermal conductivity κ_1, κ_2 ; the specific heat C_{v_1}, C_{v_2} can be expressed in the form corresponding to P_i of (1). Young's modulus is the dominant major parameter represented in the material gradation parameters only, the others are assumed in the average form for the numerical calculation of reduced stiffness. Thus the c_1 the effect only on the gradation parameter Young's modulus E_{fgm} in (10) with the relation $h^* = \sqrt{\frac{4}{3c_1}}$.

For the computed-varied values of linear k_{α} are functions of h^* , R_n and T by Hong [17], it is based on FSDT and without the function of c_1 term. For the values of nonlinear k_{α} are functions of c_1 , R_n and T by Hong [13], it is based on TSDT and without the function of h^* term. Also, a constant value $k_{\alpha} = 5/6 = 0.833333$ could be used usually in the traditional analysis.

3. Numerical results

The FGM SUS304/Si3N4 is used to study the numerical frequency of vibration under T. The constituent material 1 is SUS304 located at the lower position and material 2 is Si3N4 located at the upper position of FGM plates with a/b = 1 and $h_1 = h_2$. Values of linear k_α are used for frequency calculations of the free vibration with no external loads and no temperature difference in $\Delta T = 0$ for the TSDT of FGM plates. Preliminary considering only under four sides simply supported (SSSS) boundary conditions plate in this present study added as follows:

(a) Simply supported (SS) on x = 0 and x = a, assumed that

$$\frac{\partial u^0}{\partial x} = v^0 = w = \frac{\partial \psi_x}{\partial x} = \psi_y = 0 \tag{16}$$

(b) Simply supported (SS) on y = 0 and y = b, assumed that

$$u^{0} = \frac{\partial v^{0}}{\partial y} = w = \psi_{x} = \frac{\partial \psi_{y}}{\partial y} = 0$$
 (17)

This method is also effective for the other boundary conditions, e.g. clamp and free added as follows, and will be studied in future work.

(c) Clamp on x = 0, x = a, y = 0 and y = b, assumed that

$$u^0 = v^0 = w = \psi_x = \psi_y = 0 \tag{18}$$

(d) Free on y=0 and y=b, assumed that:

$$\frac{\partial u^0}{\partial x} = \frac{\partial v^0}{\partial y} = \frac{\partial v^0}{\partial y} = \psi_x = \frac{\partial w}{\partial x} = \psi_y = \frac{\partial w}{\partial y} = 0$$
 (19)

The present studies of vibrations are in the following time sinusoidal displacements for u^0 , v^0 , w and shear rotations ψ_x , ψ_y that forms under SSSS plate boundary conditions with amplitudes a_{mn} , b_{mn} , c_{mn} , d_{mn} , e_{mn} .

$$u^{0} = a_{mn}\cos(m\pi x/a)\sin(n\pi y/b)\sin(\omega_{mn}t)$$
 (20)

$$v^{0} = b_{mn} \sin(m\pi x/a) \cos(n\pi y/b) \sin(\omega_{mn}t)$$
 (21)

$$w = c_{mn}\sin(m\pi x/a)\sin(n\pi y/b)\sin(\omega_{mn}t) \tag{22}$$

$$\psi_x = d_{mn}\cos(m\pi x/a)\sin(n\pi y/b)\sin(\omega_{mn}t) \tag{23}$$

$$\psi_{\nu} = b_{mn} \sin(m\pi x/a) \cos(n\pi y/b) \sin(\omega_{mn} t) \tag{24}$$

where a is the length and b is the width of the plates, ω_{mn} is the natural frequency in mode shape subscript numbers m and n in the x and y directions, respectively.

It is a significant novelty with the consideration of nonlinear term c_1 in the frequency computation. By substituting (20)-(24) into dynamic equilibrium differential equations with TSDT of thick FGM plates in terms of partial derivatives of displacements and shear rotations under free vibration, thus the fully homogeneous equation can be obtained in the following form [18].

$$\mathbf{\Lambda} \mathbf{b} = \mathbf{0} \tag{25}$$

Explicit form of Eq. (25) is given in the Appendix. For the zero determinant of the coefficient matrix of (25), the polynomial equation in the fifth order of $\lambda_{\rm mn}$ can be obtained, thus the natural frequency ω_{mn} can be calculated. That is the ω_{mn} (1/s) according to mode shape numbers m and n can be computed. The subscript values m=n=1 used for the fundamental natural frequency ω_{11} . The calculated value of dimensional ω_{11} (1/s) vs. R_n for TDST and FSDT modes under linear k_α , SUS304/Si₃N₄ plate, $h^*=1.2$ mm, $\alpha/h^*=10$ and T=300K are shown in Fig. 2. The ω_{11} values in TSDT mode are smaller than that in FSDT mode. That is the values of ω_{11} are overestimated in FSDT. And the values of ω_{11} have linear with R_n in TDST.

Three non-dimensional frequency parameters f^* , ω^* and Ω are defined for the FGM plates and presented under the values effects of c_1 = 0.925925/mm²,..., 0.000001/mm² (in TSDT case) and c_1 = 0 (in FSDT case) as follows. The frequency parameter $f^* = \omega_{11}h^*\sqrt{\rho_2/E_2}$ values under the effects of c_1 values are investigated, in which ρ_2 and E_2 are the density and Young's modulus of constituent material 2, respectively. The frequency parameter $\omega^* = (\omega_{11}b^2/\pi^2)\sqrt{I_s/D_s}$ values under the effects of c_1 values are investigated, in which $I_s = \int_{-\frac{h^*}{2}}^{\frac{h^*}{2}} \rho_1 \, dz$, $D_s = \int_{-\frac{h^*}{2}}^{\frac{h^*}{2}} \overline{Q}_1 z^2 \, dz$, $\overline{Q}_1 = E_1/(1-\nu_1^2)$, where ρ_1 , E_1 and ν_1 are the density, Young's modulus and Poisson's ratio of constituent material 1, respectively. The frequency parameter $\Omega = (\omega_{11}a^2/h^*)\sqrt{\rho_1(1-\nu_1^2)/E_1}$ values under the effects of c_1 values are investigated. It is interesting to compare the present vibration values of frequency with some authors' work as shown in the Tables 1-3.

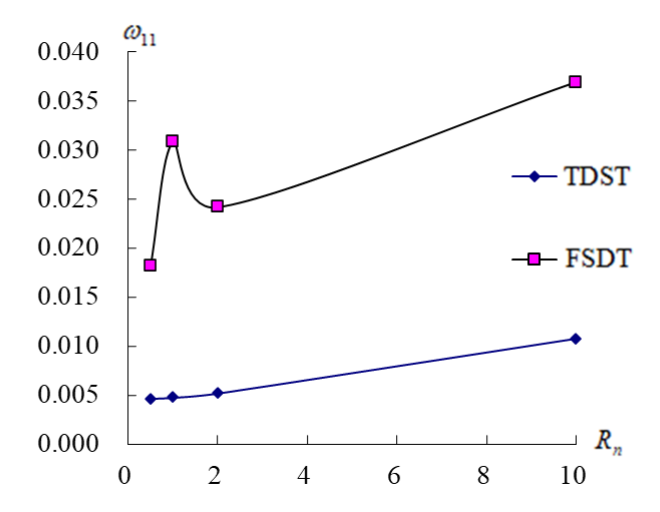


Fig. 2. ω_{11} (1/s) vs. R_n for TDST and FSDT with linear k_α and $\alpha/h^* = 10$

		f^*					
c_1 (1/mm ²)	h* (mm)	Present line	Jha et al. [19] – Al/ZrO2				
		$R_n = 0.5$	$R_n=1$	$R_n=2$	711/21/02		
0.925925	1.2	0.000285	0.000292	0.000318	-		
0.333333	2	0.003667	0.003753	0.003880	-		
0.000033	200	0.018220	0.018219	0.017421	-		
0.000014	300	0.027235	0.027235	0.027246	-		
0.000003	600	0.054278	0.054278	0.054289	-		
0.000001	900	0.081320	0.081320	0.081331	0.0839		
0.0 (FSDT)	1.2	0.001119	0.001890	0.001484	-		
0.0 (FSDT)	2	0.001687	0.001698	0.001688	-		

Table 2. Comparison of frequency ω^* for SUS304/Si₃N₄

		ω^*					
c_1 (1/mm ²)	h* (mm)	Present method, $a/h^*=10$, T=300K, linear k_{α}			Kim	Duc et al.	
		$R_n = 0.5$	$R_n=1$	$R_n=2$	2005 [20]	2017 [21]	
0.925925	1.2	0.000285	0.000292	0.000318	-	-	
0.333333	2	0.279275	0.022240	0.024256	-	-	
0.000033	200	1.387335	0.285811	0.295457	-	-	
0.000014	300	2.073790	1.387284	1.399714	-	-	
0.000003	600	4.132891	2.073762	2.074595	-	-	
0.000001	900	6.191909	4.132897	4.133752	4.1165	3.99244	
0.0 (FSDT)	1.2	0.085207	6.191933	6.192795	-	-	
0.0 (FSDT)	2	0.128498	0.143962	0.113001	-	-	

The values of f^* vs. h^* for SUS304/Si₃N₄ plate under $a/h^*=10$ and T=300K with varied linear k_α and c_1 effects are shown in Table 1, value $f^*=0.081331$ at $h^*=900$ mm, $R_n=2$ is close to $f^*=0.0839$ with Al/ZrO₂ under no T effect by Jha et al. [19] with HOSNT12 in which 12 degrees of freedom were considered for the model based on higher order shear-normal deformations theory (HOSNT). The transverse displacement field including the cubic of z for the transverse shear deformations based on higher order refined HOSNT. In the present study, the transverse displacement field is not a function of z, i.e., w = w(x, y, t). The varied values of linear k_α are also considered in present study.

The values of ω^* vs. h^* for SUS304/Si₃N₄ under $a/h^*=10$ and T=300K with varied linear k_α and c_1 effects are shown in Table 2, value $\omega^*=4.132891$ at $h^*=600$ mm, $R_n=0.5$ is close to $\omega^*=4.1165$ with $h^*=200$ mm under the vibration of $\Delta T=0$ by Kim [20]. Also, compare the present results with the analytical FSDT results $\omega^*=3.99244$ of uniform distribution (UD) in CNTRC FGM plates on elastic foundation by

Duc et al. [21]. The effect of the elastic foundation hasn't been considered in the comparative analysis of the present study.

The values of Ω vs. h^* for SUS304/Si₃N₄ under α/h^* =10 and T=700K with varied linear k_α and c_1 values effects are shown in Table 3, value Ω =5.258703 at h^* =250mm, R_n =2 is in close to Ω =5.359 under vibration of ΔT =400K by Ungbhakorn & Wattanasakulpong [22].

Table 3. Comparison of frequency Ω for SUS304/Si₃N₄

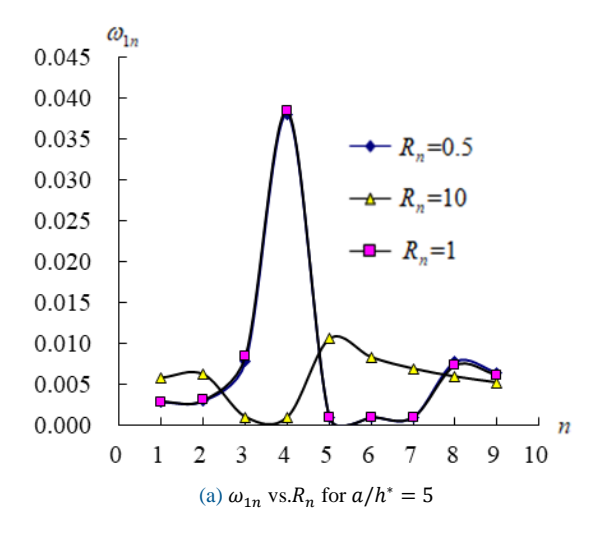
		Ω					
c_1 (1/mm ²)	h* (mm)	Present line	Ungbhakorn & Wattanasakulpong				
		$R_n = 0.5$	$R_n=1$	$R_n=2$	[22]		
0.925925	1.2	0.068259	0.069521	0.074970	-		
0.333333	2	0.895579	0.918318	0.952123	-		
0.000033	200	4.214166	4.214113	4.216926	-		
0.000021	250	5.255862	5.255844	5.258703	5.359		
0.000014	300	6.297458	6.297467	6.300357	-		
0.0 (FSDT)	1.2	0.253848	0.051565	0.057851	-		
0.0 (FSDT)	2	0.389862	1.083966	1.132692			

Table 4. Fundamental natural frequency ω_{11} for $h^*=1.2$ mm

a/h^*	R_n	c_1	ω_{11} (1/s)					
		$(1/\text{mm}^2)$	<i>T</i> =1K	T=100K	T=300K	T=600K	T=1000K	
5 (0.5	0.925925	0.002601	0.002681	0.002811	0.002902	0.002846	
3	0.3	0	0.012373	0.012851	0.013432	0.013206	0.012668	
	1	0.925925	0.002643	0.002729	0.002867	0.002951	0.002860	
	1	0	0.022565	0.031207	0.032271	0.036829	0.013303	
	2	0.925925	0.002852	0.002950	0.003102	0.003168	0.003009	
	2	0	0.022964	0.022753	0.023310	0.027759	0.015038	
	10	0.925925	0.005188	0.005470	0.005817	0.005575	0.004544	
	10	0	0.019975	0.019802	0.019823	0.020893	0.029001	
8	0.5	0.925925	0.003456	0.003573	0.003765	0.003892	0.003773	
0	0.5	0	0.018848	0.018483	0.017907	0.017266	0.017479	
	1	0.925925	0.003522	0.003648	0.003850	0.003967	0.003807	
	1	0	0.019877	0.019512	0.018765	0.018322	0.017349	
	2	0.925925	0.003814	0.003958	0.004180	0.004277	0.004029	
	2	0	0.032777	0.032918	0.034597	0.046080	0.017535	
	10	0.925925	0.007043	0.007451	0.007980	0.007693	0.006245	
	10	0	0.030320	0.030089	0.030109	0.031466	0.040707	
10	0.5	0.925925	0.004243	0.004396	0.004649	0.004818	0.004660	
10	0.5	0	0.018796	0.018587	0.018233	0.038390	0.018519	
	1	0.925925	0.004328	0.004492	0.004759	0.004917	0.004707	
	1	0	0.025488	0.028110	0.030806	0.018401	0.018175	
	2	0.925925	0.004704	0.004893	0.005190	0.005326	0.005003	
	2	0	0.039603	0.035096	0.024180	0.031271	0.018011	
	10	0.925925	0.009212	0.009847	0.010733	0.010415	0.008237	
	10	0	0.037185	0.036912	0.036918	0.038390	0.019461	

The values of ω_{11} vs. R_n with varied linear k_α and the effects of c_1 = 0.925925/mm² in TSDT and c_1 = 0 in FSDT for the SUS304/Si₃N₄ plate, h^* =1.2mm, a/h^* = 5, 8, and 10 under T=1K, 100K, 300K, 600K, and 1000K are shown in Table 4. The ω_{11} values in TSDT mode are smaller than that in FSDT mode. That is the values of ω_{11} are overestimated in FSDT and have small change values with T in TSDT.

The natural frequency ω_{mn} (1/s) vs. R_n and T of free vibration in ΔT =0 according to mode shape numbers m=1 and n from 1 to 9 for the SUS304/Si₃N₄ plate are calculated. Fig. 3 shows the values of ω_{1n} vs. R_n in FGM plate for thick a/h^* =5, 10 respectively, with the effects of varied linear k_α and c_1 =0.925925/mm² under T=300K. Generally the values of ω_{1n} are oscillating and converging to around 0.006 with values of n from 1 to 9 for a/h^* =5, R_n =0.5, 1 and 10. The greatest value of ω_{14} =0.038328/s is found, then decreasing to the value ω_{17} =0.001/s for a/h^* =5, R_n =1. The values of ω_{1n} are oscillating and diverging to around 0.05 with values of n from 1 to 9 for a/h^* =10, R_n =0.5 and 10. The smallest value of ω_{16} =0.001/s is found, then increasing to the value ω_{19} =0.054613/s for a/h^* =10, R_n =10.



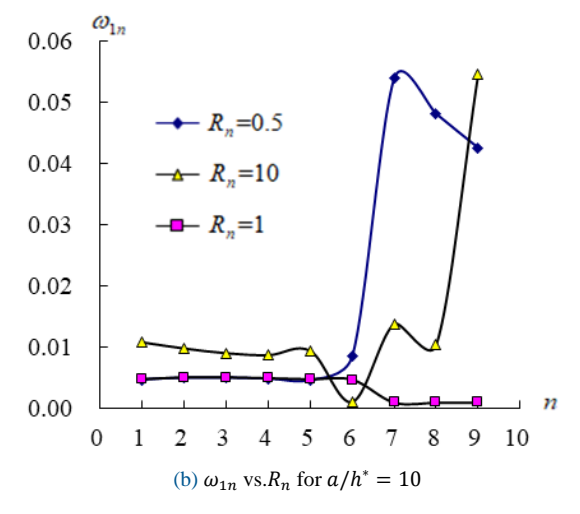


Fig. 3. ω_{1n} (1/s) vs. R_n for $a/h^* = 5$ and 10 with linear k_α

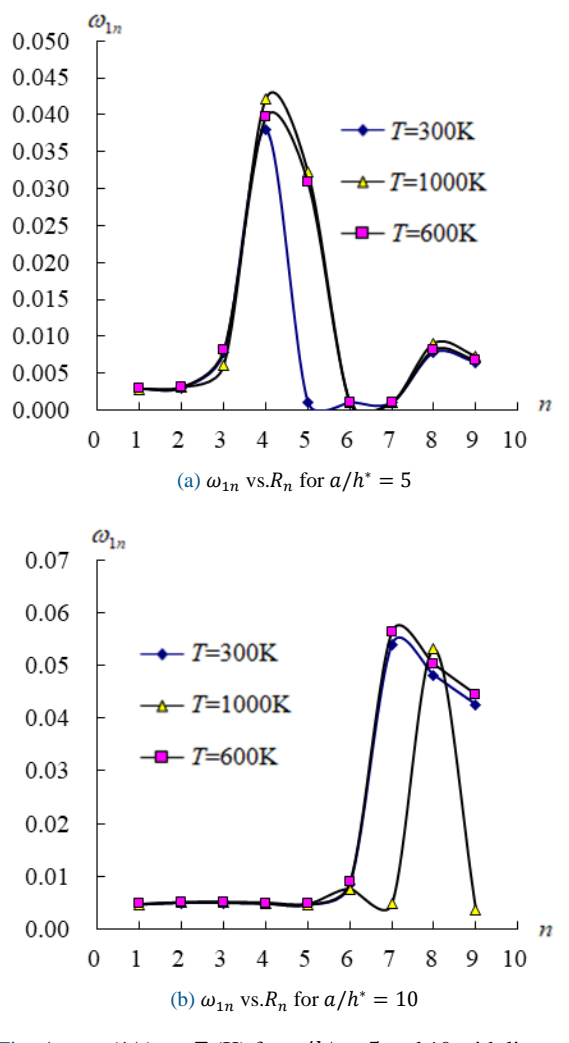


Fig. 4. ω_{1n} (1/s) vs. T (K) for $\alpha/h^* = 5$ and 10 with linear k_{α}

The Fig. 4 shows the values of ω_{1n} vs. T in FGM plate for thick $a/h^*=5$, 10 respectively, under the effects of varied linear k_{α} , $c_1=0.925925/\text{mm}^2$ and $R_n=0.5$. Generally, the values of ω_{1n} are oscillating and converging to around 0.005 with values of n from 1 to 9 for $a/h^*=5$, T=300K, 600K and 1000K. The greatest value of $\omega_{14}=0.042167/\text{s}$ is found, then decreasing to the value $\omega_{17}=0.001/\text{s}$ for $a/h^*=5$, T=1000K. The values of ω_{1n} can stand for higher temperatures on $a/h^*=10$. The greatest value of $\omega_{17}=0.056317/\text{s}$ is found for $a/h^*=10$, T=600K, thus decreasing to value $\omega_{17}=0.004738$, T=1000K.

4. Conclusions

The natural frequency ω_{mn} and frequency parameters are studied by using the polynomial equation in the fifth order of λ_{mn} in the fully homogeneous equation for the vibration of thick four sides simply supported FGM plates. Effects of nonlinear c_1 term, shear correction coefficient linear k_{α} and environment temperature T on the frequency calculations are studied. It is valuable to estimate the frequency under free vibration with the effects of nonlinear term c_1 and linear k_{α} on the TDST of FGM plates. The effects of the power-law exponent and temperature variation on the natural frequency numerical results are summarized

as follows. The ω_{11} values in TSDT are smaller than that in FSDT and the values of ω_{11} have linear variation with R_n in TDST. The values of ω_{1n} can stand on the higher temperature of 1000K for $a/h^*=10$, since the greatest value of $\omega_{17}=0.056317/s$ is found on T=600K, smaller value $\omega_{17}=0.004738$ is found on T=1000K. This method is also effective for the other boundary conditions, e.g. clamp and free boundary conditions will be studied in future work.

Conflict of interests

The author(s) declared no potential conflicts of interest with respect to the research, authorship, and/or publication of this article.

Funding

This research received no external funding.

Data availability statement

Data generated during the current study are available from the corresponding author upon reasonable request.

References

- [1] Abualnour M, Houari MSA, Tounsi A, Bedia EAA, Mahmoud SR (2018) A novel quasi-3D trigonometric plate theory for free vibration analysis of advanced composite plates. Composite Structures 184:688–697.
- [2] Mercan K, Baltacioglu AK, Civalek Ö (2018) Free vibration of laminated and FGM/CNT composites annular thick plates with shear deformation by discrete singular convolution method. Composite Structures 186:139– 153.
- [3] Vu TV, Khosravifard A, Hematiyan MR, Bui TQ (2018) A new refined simple TSDT-based effective meshfree method for analysis of through-thickness FG plates. Applied Mathematical Modelling 57:514–534.
- [4] Endo M (2017) Equivalent property between the one-half order and first-order shear deformation theories under the simply supported boundary conditions. International Journal of Mechanical Sciences 131-132:245–251.
- [5] Gupta A, Talha M (2017) Large amplitude free flexural vibration analysis of finite element modeled FGM plates using new hyperbolic shear and normal deformation theory. Aerospace Science and Technology 67:287–308.
- [6] Rezaei AS, Saidi AR, Abrishamdari M, Mohammadi MHP (2017) Natural frequencies of functionally graded plates with porosities via a simple four variable plate theory: An analytical approach. Thin-Walled Structures 120:366–377.
- [7] Singh DB, Singh BN (2017) New higher-order shear deformation theories for free vibration and buckling analysis of laminated and braided composite plates. International Journal of Mechanical Sciences 131-132:265–277.
- [8] Thai HT, Nguyen TK, Vo TP, Ngo T (2017) A new simple shear deformation plate theory. Composite Structures 171:277–285.
- [9] Senjanovi'c I, Vladimir N, Tomi'c M (2016) On new first-order shear deformation plate theories. Mechanics Research Communications 73:31–38.
- [10] Mahi A, Bedia EAA, Tounsi A (2015) A new hyperbolic shear deformation theory for bending and free vibration analysis of isotropic, functionally graded, sandwich and laminated composite plates. Applied Mathematical Modelling 39:2489–2508.
- [11] Akavci SS (2014) An efficient shear deformation theory for free vibration of functionally graded thick rectangular plates on elastic foundation. Composite Structures 108:667–676.
- [12] Jha DK, Kant T, Singh RK (2012) Higher order shear and normal deformation theory for natural frequency of functionally graded rectangular plates. Nuclear Engineering and Design 250:8–13.
- [13] Hong CC (2022) Advanced frequency analysis of thick FGM plates using third-order shear deformation theory with a nonlinear shear correction coefficient. Journal of Structural Engineering & Applied Mechanics 5(3):143–160.

- [14] Hong CC (2021) Free vibration of thick FGM plates under TSDT and thermal environment. Proceedings of Engineering and Technology Innovation 17:21–31.
- [15] Lee SJ, Reddy JN, Rostam-Abadi F (2004) Transient analysis of laminated composite plates with embedded smart-material layers. Finite Elements in Analysis and Design 40:463–483.
- [16] Shen HS (2007) Nonlinear thermal bending response of FGM plates due to heat condition. Composites Part B: eng 38:201–215.
- [17] Hong CC (2014) Thermal vibration and transient response of magnetostrictive functionally graded material plates. European Journal of Mechanics A/Solids 43:78–88.
- [18] Hong CC (2019) GDQ computation for thermal vibration of thick FGM plates by using fully homogeneous equation and TSDT. Thin-Walled Structures 135:78–88.
- [19] Jha DK, Kant T, Singh RK (2013) Free vibration response of functionally graded thick plates with shear and normal deformations effects. Composite Structures 96:799–823.
- [20] Kim YW (2005) Temperature-dependent vibration analysis of functionally graded rectangular plates. Journal of Sound and Vibration 284:531–549.
- [21] Duc ND, Lee J, Nguyen-Thoi T, Thang PT (2017) Static response and free vibration of functionally graded carbon nanotube-reinforced composite rectangular plates resting on Winkler–Pasternak elastic foundations. Aerospace Science and Technology 68:391–402.
- [22] Ungbhakorn V, Wattanasakulpong N (2013) Thermo-elastic vibration analysis of third-order shear deformable functionally graded plates with distributed patch mass under thermal environment. Applied Acoustics 74:1045– 1059.

Appendix

The following is the explicit form of Eq. (25).

where

$$\lambda_{mn} = I_0 \omega_{mn}^2,$$

$$FH_{11} = A_{11} (m\pi/a)^2 + A_{66} (n\pi/b)^2, \quad FH_{12} = (A_{12} + A_{66}) (m\pi/a) (n\pi/b),$$

$$FH_{13} = -c_1 E_{11} (m\pi/a)^3 - (c_1 E_{12} + 2c_1 E_{66}) (m\pi/a) (n\pi/b)^2, \quad FH_{14} = (B_{11} - c_1 E_{11}) (m\pi/a)^2 + (B_{66} - c_1 E_{66}) (n\pi/b)^2,$$

$$FH_{15} = (B_{12} + B_{66} - c_1 E_{12} - c_1 E_{66}) (m\pi/a) (n\pi/b),$$

$$FH_{55} = (D_{66} - 2c_1 F_{66} + c_1^2 H_{66}) (m\pi/a)^2 + (D_{22} - 2c_1 F_{22} + c_1^2 H_{22}) (n\pi/b)^2 + A_{44} - 6c_1 D_{44} + 9c_1^2 F_{44}$$